

# MODELLING OF CHAOTIC BEHAVIOR IN POWER SYSTEMS USING RECURRENT NEURAL NETWORKS

*by I Made Ginarsa*

---

**Submission date:** 21-Nov-2022 01:15PM (UTC+0700)

**Submission ID:** 1960071642

**File name:** Proceedings\_ICACIA\_2008\_Part8.pdf (175.84K)

**Word count:** 4120

**Character count:** 19953

## MODELLING OF CHAOTIC BEHAVIOR IN POWER SYSTEMS USING RECURRENT NEURAL NETWORKS

16 I Made Ginarsa  
Electrical Engineering, Mataram University

Mataram, Indonesia  
e-mail: [kadegkin@elect-eng.its.ac.id](mailto:kadegkin@elect-eng.its.ac.id)

10 Adi Soeprijanto, Mauridhi Hery Pumomo  
Electrical Engineering,  
Institute Technology Sepuluh Nopember  
Surabaya, Indonesia  
e-mail: [adisup@ee.its.ac.id](mailto:adisup@ee.its.ac.id), [hery@ee.its.ac.id](mailto:hery@ee.its.ac.id)

**Abstract** This paper presents the intensely studied route to chaotic oscillation in power systems. By using a three-bus simple power system, a route was found to cause chaotic behavior in the power systems which are evaluated, illustrated, and discussed in this study. Furthermore, chaotic behavior by using recurrent neural networks (RNN) and exact models are compared. In particular, we have proposed that RNN can be trained by using it on both the present input and past output, using back-propagation algorithm with adaptive learning rate and momentum. Performance of learning rate with momentum is better than learning rate without momentum. The appearance of chaotic behavior in a power system is already proven and can be modeled by using the RNN. A chaotic behavior is detected by a strange attractor (a chaotic attractor) in the phase-plane. The largest mean squared error (MSE) was observed to be 7.8296% obtained on the rotor speed  $\omega$  at a disturbance of 1.7003 rad/sec. On the contrary, the least MSE was 0.0407% obtained on load voltage at disturbance 1.600 rad/sec.

**Key words:** Power systems, chaotic behavior, recurrent neural networks (RNN), chaotic attractor, phase-plane.

### I. INTRODUCTION

Chaotic phenomena are the form of undeterministic oscillations that exist in the deterministic systems. Electric power system is a nonlinear system with many apparatus having inheritance nonlinearity. Chiang et al. built the voltage collapse model and presented both the physical explanations and computational considerations of this model. Static and dynamic models are used to explicate the type of voltage collapse, where the static is used before a saddle-node bifurcation and the dynamic model is employed after the bifurcation [1]. The Lyapunov exponent, measuring how rapidly the two nearby trajectories separate from one another within the state space and broadband spectrum, is used to confirm the observation [2]. Within the range of loading conditions, the sensitive-dependence feature of chaotic behavior makes the power system unpredictable after a finite time. Also, within the range, the effectiveness of any control scheme is in doubt should be re-evaluated based on the state vector information. Furthermore, nonlinear phenomena, including bifurcations and chaos, occur in the power systems model exhibiting voltage collapse. The presence of various nonlinear phenomena is found to be a crucial factor in the inception of voltage collapse in this model. Moreover, the problem of controlling in the presence of these linear phenomena is addressed. The bifurcation-control approach modifies the bifurcations and suppresses chaos [3][4]. The relationships between chaos and power system instability were studied by Yu et al. [5]. The existence of chaos in power

systems owing to the disturbance energy at rotor speed has been studied previously [6]. A scheme of chaos utility is used in the electrical systems for smelting base on chaos control. Zhao-Ming et al. demonstrated that the chaotic steel-smelting oven regulated its heating current according to the chaos control theory [7]. Control system using a neural-network controller is presumed to stabilize the unstable focus points of two-dimensional chaotic systems. However, Konishi and Kokame stated that the control system does not require such knowledge [8]. Various studies were carried out to control transient chaos, such as the one by Damala and Ying-Cheng, who attempted to control transient chaos in power systems using data-time series [9]. Furthermore, Strategies of controlling chaos in the process plants were tested on a discrete chaotic system of Henon map [10]. In this study, we focused on the cause of chaotic oscillation in power systems and its model, by using recurrent neural network (RNN) models. The main reason for using RNN is that it can be trained by using it on both the present input and past output, and also because of its simple form (an Elman RNN).

In Section II, the power system models used in this research are presented, followed by the description of RNN model used in this study Section III. The chaotic sensitivity to initial condition and analysis of the chaotic behavior are presented in Sections IV and V, respectively, followed by the conclusions in the last section.

### II. POWER SYSTEMS MODEL

Synchronous machine is modeled by voltage  $E'$  behind direct reactance  $X_d'$ . Its magnitude is assumed to remain constant at the pre-disturbance value, as shown in Fig. 1(a). De Mello and Concordia as well as Padiyar and Kundur derived this model connected to infinite bus [11][12]. However, saturation and stator resistance are neglected, and the system condition is balanced with static load. The block-diagram for the mechanism of single machine connected to infinite bus is shown in Fig. 1(b).

The machine is connected to infinite bus and the supplying load. Armature current flows from the machine to the load. This current causes electric torque on the stator winding, and vice versa. The mechanical torque is produced by flux on the rotor winding. When the rotor speed is constant, it will follow the synchronous speed. When there is an imbalanced energy, the rotor speed may be accelerated or decelerated and causing the swing equation. Swing equation is represented as follows:

$$H \frac{\partial^2 \delta}{\partial t^2} + D \omega = T_a = T_m - T_e \quad (1)$$

where  $D$  and  $\omega$  are damping constant and rotor speed, respectively. Equation (1) is a basic equation for mode mechanical machine, which can be modified furthermore to Eq. (2) and Eq. (3).

$$\Delta \dot{\delta} = \omega_B \Delta \omega \quad (2)$$

$$\Delta \dot{\omega} = \frac{1}{M} (\Delta T_m - \Delta T_e - D \Delta \omega) \quad (3)$$

where  $\Delta T_m$ ,  $\Delta T_e$ ,  $\Delta \delta$ ,  $\Delta \omega$ ,  $D$ , and  $M$  are mechanical torque, electrical torque, power angle, rotor speed, damping constant, and inertia constant, respectively.

The system was developed from the work of Chiang et al. and Yu et al. [2][5] (Fig.2) and is regarded as a synchronous machine supplying power to a local dynamic load-shunt with a capacitor (Bus 2) connected by a weak tie-line to the external system (Bus 3). The system equations are:

$$\dot{\delta} = \omega \quad (4)$$

$$\dot{\omega} = 16.667 \sin(\delta_L - \delta + 0.087)V_L - 3.333.d.\omega + 1.881 \quad (5)$$

$$\dot{\delta}_L = 496.872V_L^2 - 166.667 \cos(\delta_L - \delta - 0.087)V_L - 93.333V_L \quad (6)$$

$$- 666.667 \cos(\delta_L - 0.209)V_L - 33.333Q_{ld} + 43.333$$

$$\dot{V}_L = -78.764V_L^2 + 26.217 \cos(\delta_L - \delta - 0.012)V_L + 14.523V_L + 104.869 \cos(\delta_L - 0.135) - 5.229Q_{ld} - 7.033 \quad (7)$$

$\delta$ ,  $\omega$ ,  $d$ ,  $Q_{ld}$ ,  $\delta_L$ ,  $V_L$  are power angle, rotor speed, damping constant, reactive load, voltage angle, and voltage magnitude at load bus, respectively. Equations (4)-(7) can be simplified into a uniform equation, as shown in Eq. (8).

$$\dot{x} = f(x, \lambda), \quad x \in R^n, \lambda \in R^p \quad (8)$$

where  $x$  denotes the vector-state variables and  $\lambda$  signifies the vector of parameters. The state variables are  $x = [\delta, \omega, \delta_L, V_L]^T$ , where superscript  $T$  denotes the transpose of the associate vector.

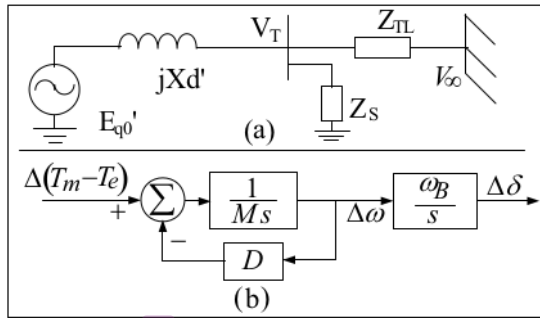


Figure 1. Synchronous machine connected to infinite bus.  
(a) Circuit equivalent. (b) Block diagram-mode mechanics.

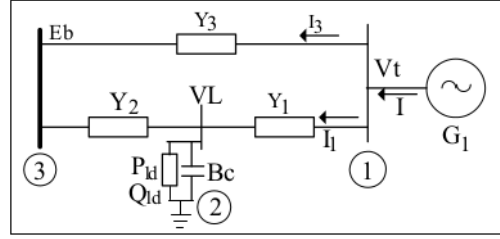


Figure 2. One-line diagram of power system with three buses.

TABLE I. THE SYSTEM PARAMETERS [5].

$Y_1$	$Y_2$	$Y_3$	$\phi$	$\phi$	$\phi$	$E_b$	
4.975	1.658	0.01	-1.471	-1.471	-1.4	1.0	
$E_m$	$X_d$	$X_q$	$X_d'$	$X_q'$	$T_{d0}'$	$T_{q0}'$	
1.0	1.79	1.71	0.169	0.23	4.3	0.85	
$H$	$\omega_B$	$d$	$P_d$	$Q_d$	$p_L$	$q_L$	$B_c$
2.89	377	0.05	0.4	0.8	0.24	-0.02	0.2
$p_2$	$q_2$	$p_3$	$q_3$	$Q_{ld}$	$P_{ld}$	$K_A$	$T_A$
1.7	-1.866	0.2	1.6	0	0	200	0.05

### III. RECURRENT NEURAL NETWORKS

Recurrent Elman network commonly is a two-layer network with feedback from the first-layer output to the first-layer input. This recurrent connection allows the Elman network to both detect and generate the time-varying patterns. A two-layer Elman network is shown in Fig. 3. The Elman network has tangent sigmoid (tansig) neurons in its hidden (recurrent) layer and pure linear (purelin) in its output layer. The Elman network differs from the conventional two-layer networks in that the first layer has a recurrent connection. The delay in this connection stores the values from the previous time-step, which can be used in the current time-step. Thus, even if two Elman networks with the same weight and bias are given identical inputs at a given time-step, their outputs can be different owing to the different feedback states. As the network can store the information for future reference, it can understand the temporal pattern as well as spatial patterns [15][16][17][18]. The Elman networks can be trained to respond and generate both kinds of patterns.

$$\begin{aligned} a^1(n) &= \text{tansig}(IW_{1,1}p + LW_{1,1}a^1(n-1) + b_1) \\ a^2(n) &= \text{purelin}(LW_{2,1}a^1(n) + b_2) \end{aligned} \quad (9)$$

In this study, the architecture 4:8:8:4 RNN was used, where  $p$ ,  $a^1(n)$ ,  $a^2(n)$ ,  $IW_{1,1}$ ,  $LW_{1,1}$ ,  $LW_{1,2}$ ,  $b_1$ , and  $b_2$  are vector input, recurrent-layer output, purelin-layer output, weight first-layer, weight hidden layer back to first-layer, weight hidden layer to output layer, and biases, respectively. The RNNs were developed with 1000 data points. Tansig and purelin activation function were used at hidden and output layer, respectively. Data time series were obtained from mathematical (exact) model of Eq. (4)–Eq. (7), respectively. The network performance was measured by mean square error (MSE). Mathematically, MSE can be expressed in the form of an equation as follows.

$$MSE = \frac{1}{k} \left[ \sum_{i=1}^k (\hat{x}_n - x_n)^2 \right] \quad (10)$$

where  $k$ ,  $x_n$ , and  $\hat{x}_n$  are the size of data, input, and estimation of  $n$ th data.

**IV. CHAOTIC SENSITIVITY TO INITIAL CONDITIONS**

The chaos definition and its properties have been given by Devaney and Alligood et al. [13][14]. Sensitivity of the initial condition is one type of chaos properties. It is described by the existing route to chaotic behavior in the power systems caused by sensitivity of initial-condition rotor speed ( $\omega_0$ ). Rotor speed ( $\omega_0$ ) in the power systems is presented by disturbing energies (DE). Kinetic energy disturbance is exclusively related to the rotor speed. If DE is larger, then it will result in larger rotor speed. When  $DE < 1.3824$  rad/sec ( $\omega_0 < 1.3824$  rad/sec), the power system can converge to a stable equilibrium point. If DE increases, the convergence becomes more difficult. At  $\omega_0 = 1.3825$  rad/sec, the power systems will route to a chaotic behavior in a longer duration. At a range of 1.3825–17003 rad/sec, the final states are controlled by a chaotic behavior. Furthermore, if the rotor is  $> 1.7004$  rad/sec, then the system will undergo monotonic divergence or collapse. It has been proven that chaotic behavior in the power systems caused by injecting energy results in unexpected disturbances.

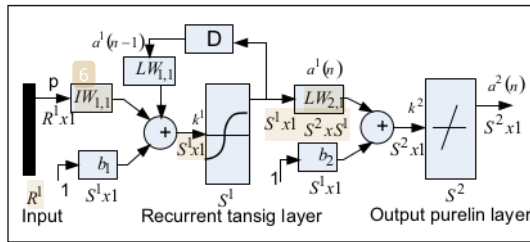


Figure 3. Block diagram of RNN [18].

**TABLE II. SYSTEM CONDITIONS WITH DIFFERENT INITIAL ROTOR SPEEDS ( $\omega_0$ ) [6].**

$\omega_0$ (rad/sec)	Time (sec)	Final state	Time response
0.5	1000	Equilibrium point	Fig. 4(a)
1.3824	1000	Equilibrium point	Fig. 4(b)
1.3825	1000	Chaotic	Fig. 5(a)
1.7003	1000	Chaotic	Fig. 5(b)
1.7004	10	Divergence	–

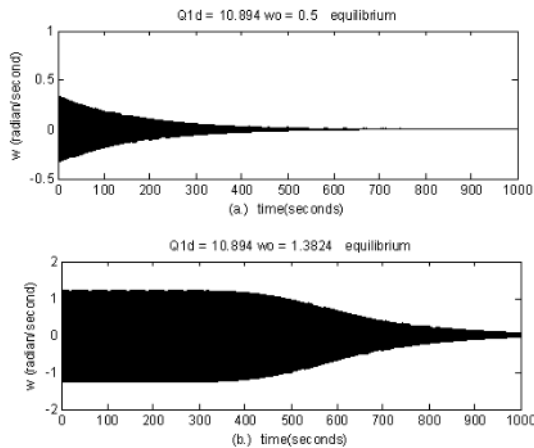


Figure 4. Simulation results with equilibrium point state.

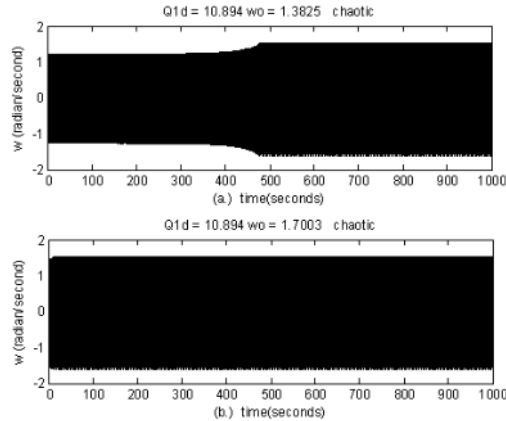


Figure 5. Simulation results with chaotic state.

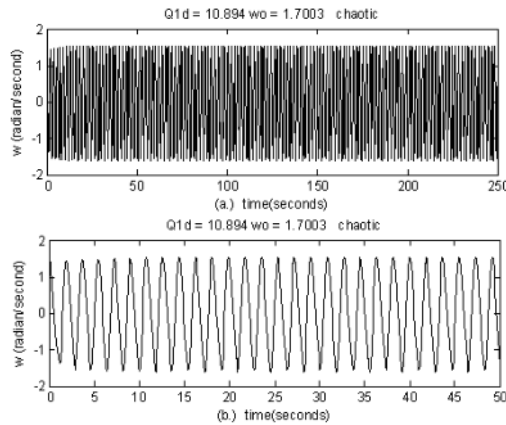


Figure 6. (a) Magnification of Fig. 5 between 0 and 250 sec. (b) Magnification of Fig. 5 between 0 and 50 sec.

**V. RESULTS AND ANALYSIS**

The RNN initial simulation parameters were obtained as follows: 0.17 for learning rate train parameter, 1.2 for increment learning rate, 0.6, and 0.75 for decrement learning rate and momentum learning rate, respectively. The training performance of RNN using adaptive learning rate with momentum is shown in Table III.

The training process was organized as follows: the RNN performances (MSE) were obtained as  $14.7001 \times 10^{-4}$  and  $4.2209 \times 10^{-4}$  at a disturbance of  $\omega_0 = 0.5$  rad/sec for algorithm back-propagation adaptive learning rate (traingda) and back-propagation learning rate algorithm with momentum (traingdx), respectively. Subsequently, at the disturbance of  $\omega_0 = 1.3825$  and 1.7003 rad/sec, the performances (MSE) for algorithm back-propagation adaptive learning rate (traingda) and algorithm back-propagation adaptive learning rate with momentum (traingdx) were  $16.8361 \times 10^{-4}$  and  $4.6115 \times 10^{-4}$ , and  $17.4185 \times 10^{-4}$  and  $4.9442 \times 10^{-4}$ , respectively. Furthermore, during the training process the best performance (MSE) was obtained as  $4.2209 \times 10^{-4}$  at the disturbance of  $\omega_0 = 0.5$  rad/sec.



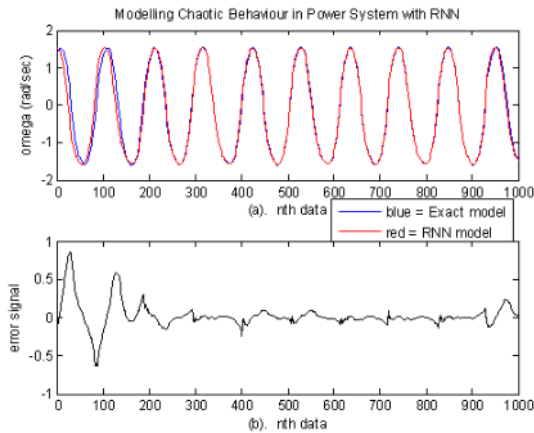


Figure 7. Rotor speed ( $\omega$ ) time response at chaotic state at  $\omega_0 = 1.7003$  rad/sec. (a) Blue = exact; red = RNN. (b) Error signal.

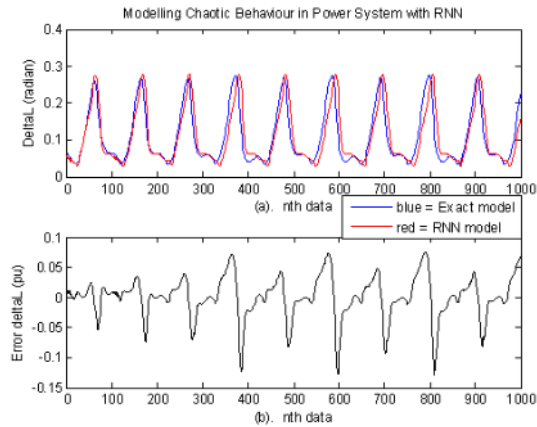


Figure 8. Voltage angle ( $\delta_L$ ) time response at chaotic state at  $\omega_0 = 1.7003$  rad/sec. (a) Blue = exact; red = RNN. (b) Error signal.

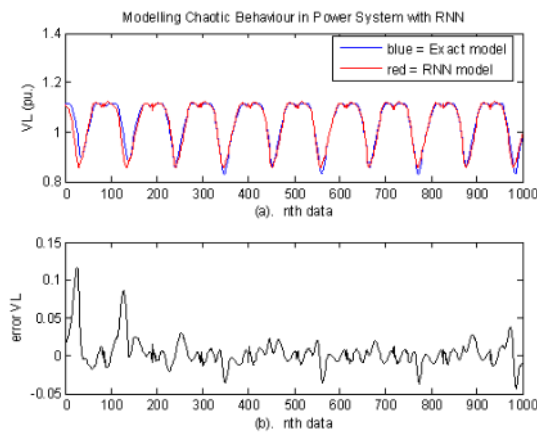


Figure 9. Voltage magnitude ( $V_L$ ) time response at  $\omega_0 = 1.7003$  rad/sec. (a) Blue = exact; red = RNN. (b) Error signal  $V_L$ .

TABLE III. PERFORMANCES TRAINING ALGORITHM USING LEARNING RATE WITH MOMENTUM.

$\omega_0$ (rad/sec)	Training Time (sec $\times 10^2$ )		Performances MSE ( $\times 10^{-4}$ )	
	traingda	traingdx	Traingda	traingdx
0.5	69.3861	37.403	14.7001	4.2209
1.3824	68.3250	42.342	17.2014	4.9080
1.3825	67.3329	36.750	16.8361	4.6115
1.7003	70.5781	41.840	17.4185	4.9442

Figures 7–9 illustrate the result of time response by exact and RNN models. Figure 7(a) shows the rotor speed ( $\omega$ ) time response which is oscillated by the disturbance occurring at  $\omega_0 = 1.7003$  rad/sec. Rotor speed oscillations for exact and RNN exist in range from  $-1.6052$  to  $1.5679$  rad/sec and  $-1.5411$  to  $1.6045$  rad/sec, respectively. The difference in both these signals, known as rotor speed error signal, is shown in Fig. 7(b), where at this moment, the rotor speed exhibits chaotic behavior.

The voltage angle ( $\delta_L$ ) at Bus 2 is affected by disturbing rotor speed at the generator bus ( $\omega_0 = 0.5$  rad/sec). The oscillation on the voltage angle occurs at the generator bus in 735 sec. Furthermore, this oscillation decreased gradually and route to equilibrium state (fixed point) at the point of 0.1128 rad and 0.1116 rad for exact and RNN model, respectively. The error signal is measured by MSE (MSE = 3.8193%). This result is shown in Table IV.

Oscillation voltage angle was observed to increase at the disturbance 1.3824, 1.3825, 1.600 and, 1.7003 rad/sec for the exact model with amplitude in the ranges from 0.0600 to 0.1995 rad, 0.0351 to 0.2730 rad, 0.0345 to 0.2748 rad and 0.0340 to 0.2756 rad, respectively; while the oscillation for the RNN model are in the ranges from 0.0501 to 0.1879 rad, 0.0460 to 0.2644 rad, 0.0332 to 0.2618 rad, and 0.0342 to 0.2613 rad, respectively. This oscillation occurred for a longer duration. The voltage angle time-response occurring at disturbance  $\omega_0 = 1.7003$  rad/sec is shown in Fig. 8.

At disturbance  $\omega_0 = 0.5$  rad/sec, the voltage magnitude was oscillated in 410 sec. Furthermore, it decreased gradually route to equilibrium state (fixed point) at point 1.095 and 1.008 pu for exact and RNN model, respectively. By increasing the disturbance at  $\omega_0 = 1.3824$  rad/sec, the voltage magnitude was oscillated for a longer duration in the range from 0.9967 to 1.1207 pu for exact model, and subsequently, the amplitude was reduced and fixed point at 1.1095 pu (1520 sec).

On the contrary, when the disturbance was increased up to 1.3825, 1.600, and 1.7003 rad/sec, the voltage magnitude oscillated for the exact model with increasing amplitude in the ranges from 0.8307 to 1.1220 pu, 0.8285 to 1.1118 pu, and 0.8290 to 1.1119 pu, respectively; whereas, the oscillation for the RNN model were in the ranges from 0.8497 to 1.1158 pu, 0.8580 to 1.1235 pu, and 0.8642 to 1.1185 pu, respectively.

State trajectory (orbit) of the  $\omega$  vs.  $\delta$  is shown in Fig. 10, where the circles are made by themselves with boundary ranges from  $-1.6011$  to  $+1.5535$  rad/sec, and  $-0.1165$  to  $+0.7583$  rad for  $\omega_{min}$  to  $\omega_{max}$  and  $\delta_{min}$  to  $\delta_{max}$ , respectively. State trajectory for the RNN model was made in the ranges  $-1.6020$  to  $+1.5524$  rad/sec and  $-0.1645$  to  $+0.7598$  rad. This form is known as the strange attractor (chaotic attractor).

The strange attractors are made by  $\delta_L$  vs.  $V_L$  state trajectories, as shown in Fig. 11 at coordinates in the ranges from 0.0345 to 0.2748 rad and 0.8285 to 1.1118 pu for  $\delta_{L,max}$  to  $\delta_{L,min}$  and  $V_{L,max}$  to  $V_{L,min}$ , respectively; subsequently, the RNN model in the ranges from 0.0332 to 0.2618 rad and 0.8280 to 1.1235 pu for  $\delta_{L,max}$  to  $\delta_{L,min}$  and  $V_{L,max}$  to  $V_{L,min}$ , respectively.

Furthermore, existence of the chaotic attractors is also depicted in Figs. 12 and 13 for  $\omega_0 = 1.7003$  rad/sec. Figure 12 illustrates  $\omega$  vs.  $\delta$  state trajectories at coordinates from  $-1.6052$  to  $+1.5679$  rad/sec and  $-0.1157$  to  $+0.7601$  rad for  $\omega_{min}$  to  $\omega_{max}$  and  $\delta_{min}$  to  $\delta_{max}$ , respectively. The results from the RNN model are depicted by the red circles at coordinates from  $-1.5410$  to  $+1.6045$  rad/sec and  $-0.1345$  to  $+0.7457$  rad for  $\omega_{min}$  to  $\omega_{max}$  and  $\delta_{min}$  to  $\delta_{max}$ , respectively.

TABLE IV. SYSTEM STATE WHEN VARIATION OF DISTURBANCE ( $\omega_0$ ) IS APPLIED.

$\omega_0$ and Model	$\delta$ (rad)	$\omega$ (rad/sec)	$\delta_L$ (rad/sec)	$V_L$ (pu)
<b>0.5 exact</b>	Eq 0.3095	Osc-0.2104 to 0.2123	Eq 0.1128	Eq 1.095
<b>RNN</b>	Eq 0.3194	Osc-0.2048 to 0.2090	Eq 0.1116	Eq 1.008
<b>MSE (%)</b>	0.2636	6.1792	3.8193	6.9051
<b>1.3824 exact</b>	Osc-0.0245 to 0.6160	Osc-1.1546 to 1.1049	Osc 0.0600 to 0.1995	Osc 0.9967 to 1.1207
<b>RNN</b>	Osc-0.0256 to 0.6165	Osc-1.0246 to 1.0049	Osc 0.0501 to 0.1879	Osc 0.9970 to 1.1135
<b>MSE (%)</b>	3.9625	6.3023	0.2040	0.1154
<b>1.3425 Exact</b>	Osc-0.1156 to 0.7578	Osc-1.5711 to 1.5142	Osc 0.0351 to 0.2730	Osc 0.8307 to 1.1220
<b>RNN</b>	Osc-0.1148 to 0.7510	Osc-1.5734 to 1.5165	Osc 0.0460 to 0.2644	Osc 0.8497 to 1.1158
<b>MSE (%)</b>	0.68	0.23	1.09	1.90
<b>1.6000 Exact</b>	Osc-0.1165 to 0.7583	Osc-1.6011 to 1.5535	Osc 0.0345 to 0.2748	Osc 0.8285 to 1.1118
<b>RNN</b>	Osc-0.1645 to 0.7598	Osc-1.6020 to 1.5524	Osc 0.0332 to 0.2618	Osc 0.8580 to 1.1235
<b>MSE (%)</b>	0.2163	2.8779	0.0460	<b>0.0407</b>
<b>1.7003 Exact</b>	Osc-0.1157 to 0.7601	Osc-1.6052 to 1.5679	Osc 0.0340 to 0.2756	Osc 0.8290 to 1.1119
<b>RNN</b>	Osc-0.1345 to 0.7457	Osc-1.5410 to 1.6045	Osc 0.0342 to 0.2613	Osc 0.8642 to 1.1185
<b>MSE (%)</b>	1.0522	<b>7.8296</b>	0.1284	0.1470

Note: Eq = equilibrium point (fixed point); Osc = oscillation.

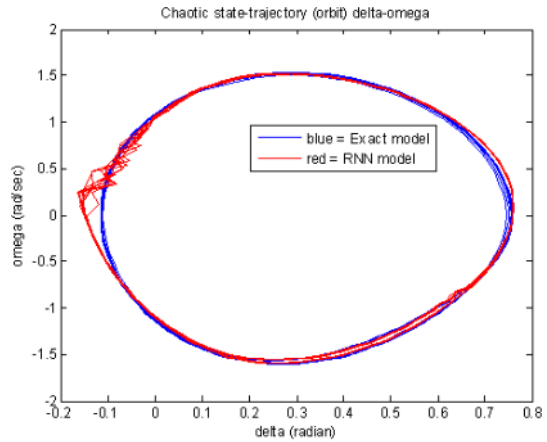


Figure 10.  $\omega$ - $\delta$  State trajectory with disturbance at  $\omega_0 = 1.600$  rad/sec.

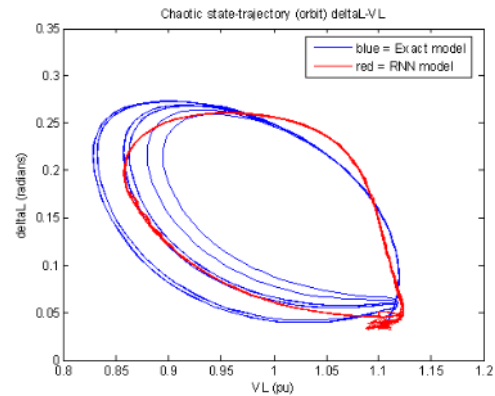


Figure 11.  $\delta_L$ - $V_L$  State trajectory when applied disturbance at  $\omega_0 = 1.6000$  rad/sec.

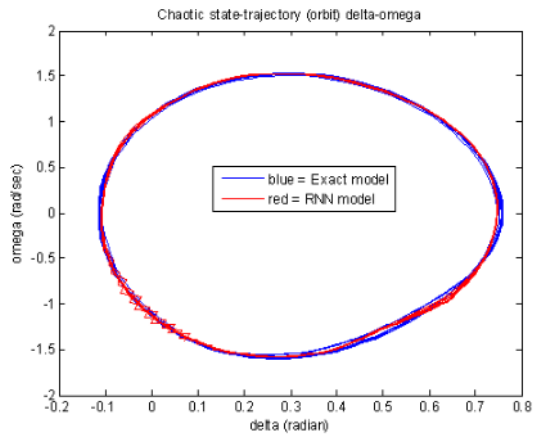


Figure 12.  $\omega$ - $\delta$  State trajectory when applied disturbance at  $\omega_0 = 1.7003$  rad/sec.

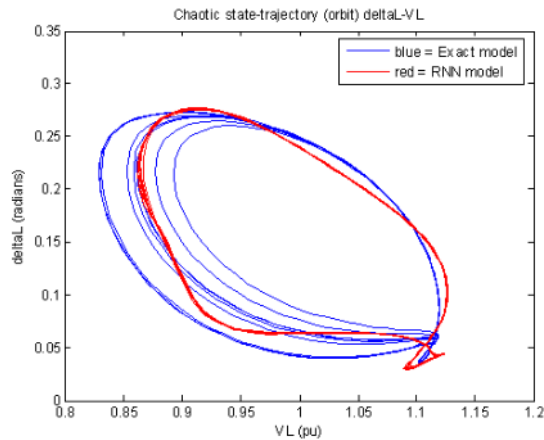


Figure 13.  $\delta_L$ - $V_L$  State trajectory when applied disturbance at  $\omega = 1.7003$  rad/sec.

Figure 13 illustrates  $\delta_L$  vs.  $V_L$  state trajectories at coordinates 0.0340 to 0.2756 rad and 0.8290 to 1.1119 pu for  $\delta_{Lmax}$  to  $\delta_{Lmin}$  and  $V_{Lmax}$  to  $V_{Lmin}$ , respectively. The state trajectories RNN model is depicted by the red points at coordinates 0.0342–0.2613 rad and 0.8642–1.1185 pu for  $\delta_{Lmax}$  to  $\delta_{Lmin}$  and  $V_{Lmax}$  to  $V_{Lmin}$ , respectively. The complete results are tabulated in Table IV.

The RNN performance can be measured by difference signal output from exact and RNN models. From Table IV we can observe that the largest MSE is 7.8296% obtained on speed rotor  $\omega$  at disturbance 1.7003 rad/sec. On the contrary, the least MSE is 0.0407% obtained on the load angle at disturbance 1.600 rad/sec. Thus, it is proven that chaotic behavior in power systems can be modeled by RNN.

## VI. CONCLUSIONS

In this paper, extensive investigation was carried out on the chaotic oscillation by exact and RNN model. The training by using adaptive learning rate, both with and without momentum was compared, and the adaptive learning rate performance with momentum was found to be better. Chaotic behaviors were detected in the power systems by the chaotic attractors both at the power angle-rotor speed and magnitude-angle voltage state-trajectories in the phase-plane. The largest MSE is 7.8296% obtained on the rotor speed  $\omega$  at disturbance 1.7003 rad/sec. On the contrary, the least MSE was 0.0407% obtained on the load voltage at disturbance 1.600 rad/sec.

## FUTURE WORK

Recently, chaotic behavior in power systems has been the topic of interest in research. The chaotic behavior can be reduced from power systems by properly applying the control strategy.

## REFERENCES

- [1] H-D. Chiang, et al., "On Voltage Collapse in Electric Power Systems", *IEEE Transactions on Power Systems*, Vol. 5, No.2, May 1990.
- [2] H-D. Chiang, P.P. Varaiya, F.F. Wu and M. G. Lauby, "Chaos in a Simple Power System", *IEEE Transactions on Power Systems*, Vol. 8, No. 4, November 1993.

- [3] H. O. Wang, Control of Bifurcation and Routes to Chaos in Dynamical System, Thesis Report Ph.D, Institute for Systems Research, The University of Maryland, USA, 1993.
- [4] H. O. Wang, E. H. Abed and A.M.A. Hamdan, "Bifurcations, Chaos, and Crises in Voltage Collapse of a Model Power System", *IEEE Transactions on Circuit and Systems I: Fundamental, Theory and Applications*, Vol. 41, No.3, March 1994.
- [5] Y. Yu, H. Jia, P. Li, and J. Su, "Power System Instability and Chaos", 14<sup>th</sup> PSCC, Sevilla, 2002.
- [6] I M. Ginarsa, A. Soeprijanto and M. H. Purnomo, "Implementasi Model Klasik untuk Identifikasi Chaotic dalam Sistem Tenaga Listrik Akibat Gangguan Energi", Proceedings of the 9<sup>th</sup> Seminar on Intelligent Technology and Applications (SITIA 2008), Surabaya, 8<sup>th</sup> May 2008.
- [7] L. Zhao-Ming, L. Zuo-Jun, S. He-xu, L. Hong-Xun, "Control and Application of Chaos in Electrical System", Proceedings of the Fourth International Conference on Machine Learning and Cybernetics, Guangzhou, 18-21 August 2005.
- [8] K. Konishi and H. Kokame, "Stabilizing and Tracking Chaotic Orbits Using a Neural Network", International Symposium on Nonlinear Theory and Its Applications (NOLTA'95), Las Vegas, U.S.A, December 10-14, 1995.
- [9] M. Dhamala and L. Ying-Cheng, "Controlling Transient Chaos in Deterministic flows with Applications to Electric Power Systems and Ecology", *Physical Review E*, Vol. 59, No.2, February 1999.
- [10] J. Krishnaiah, C.S. Kumar, and M.A. Faruqi, "Modelling and Control of Chaotic Processes through Their Bifurcation Diagrams Generated with The Help of Recurrent Neural Network Models : Part 1-Simulation Studies", *Journal of Process Control*, Elsevier, 2006, pp.53-66.
- [11] K.R. Padiyar, Power System Dynamic Stability and Control, John Wiley & Sons (Asia) Pte Ltd, Singapura, 1984.
- [12] P. Kundur, Power System Stability and Control, EPRI, McGraw-Hill, New York, 1994.
- [13] R.L. Devaney, A First Course in Chaotic Dynamical Systems: Theory and Experiment, Addison-Wesley Publishing Company Inc, New York, 1992.
- [14] K.T. Alligood, T.D. Sauer and J.M. Yorke, Chaos: An Introduction to Dynamical Systems, Springer-Verlag, New York, 2000.
- [15] O.M. Omidvar and D. L. Elliot, Neural Systems for Control, Academic Press, February 1997.
- [16] L.R. Medsker, and L.C. Jain, Recurrent Neural Networks: Design and Applications, CRC Press, Boca Raton, 2001.
- [17] M. Norgaard, Neural Network Based System Identification Toolbox: for Use with Matlab, Department of Automation, Department of Mathematical Modelling, Technical University of Denmark.
- [18] -----, MATLAB Version 7.04 : The Language of Technical Computing, The Matworks Inc, 2005.

# MODELLING OF CHAOTIC BEHAVIOR IN POWER SYSTEMS USING RECURRENT NEURAL NETWORKS

## ORIGINALITY REPORT

17%

SIMILARITY INDEX

8%

INTERNET SOURCES

14%

PUBLICATIONS

7%

STUDENT PAPERS

## PRIMARY SOURCES

- 1** Yixin Yu, Hongjie Jia, Peng Li, Jifeng Su. "Power system instability and chaos", Electric Power Systems Research, 2003 **3%**  
Publication
- 2** [matlab.izmiran.ru](http://matlab.izmiran.ru) **2%**  
Internet Source
- 3** Thiery, F.. "Integration of neural networks in a geographical information system for the monitoring of a catchment area", Mathematics and Computers in Simulation, 20080107 **2%**  
Publication
- 4** Hsiao-Dong Chiang, Chih-Wen Liu, P.P. Varaiya, F.F. Wu, M.G. Lauby. "Chaos in a simple power system", IEEE Transactions on Power Systems, 1993 **1%**  
Publication
- 5** [uad.portalgaruda.org](http://uad.portalgaruda.org) **1%**  
Internet Source



6

Internet Source

1 %

7

L. Fekih-Ahmed. "On voltage collapse in electric power systems", Conference Papers Power Industry Computer Application Conference, 1989

Publication

1 %

8

Hong-Xun Liu. "Control and Application Of Chaos in Electrical System", 2005 International Conference on Machine Learning and Cybernetics, 2005

Publication

1 %

9

Hongjie Jia, Yixin Yu, Peng Li, Jifeng Su. "Torus bifurcation and chaos in power systems", Proceedings. International Conference on Power System Technology, 2002

Publication

1 %

10

Mochamad Hariadi, I. G. P. Asto Buditjahjanto, Mauridhi Hery Purnomo. "Decision Support Based on Integration of Fuzzy Clustering and Multiobjective Optimization Problem for Non Player Character in Business Game", 2009 International Conference of Soft Computing and Pattern Recognition, 2009

Publication

1 %

11

[cogprints.org](http://cogprints.org)

Internet Source

&lt;1 %

12

Submitted to Udayana University

Student Paper

&lt;1 %

13

Submitted to University of Birmingham

Student Paper

&lt;1 %

14

E.A. Mohamed. "A robust system stabilizer configuration using artificial neural network based on linear optimal control (student paper competition)", CCECE 2003 - Canadian Conference on Electrical and Computer Engineering Toward a Caring and Humane Technology (Cat No 03CH37436) CCECE-03, 2003

Publication

&lt;1 %

15

Keiji Konishi, Hideki Kokame. "Control of chaotic systems using an on-line trained linear neural controller", Physica D: Nonlinear Phenomena, 1997

Publication

&lt;1 %

16

[internationalscienceindex.org](http://internationalscienceindex.org)

Internet Source

&lt;1 %

17

Jia Hongjie, Yu Yixin, Yu Xiaodan, Huang Chunhua, Zhang Pei. "Three routes to chaos in power systems", Canadian Conference on Electrical and Computer Engineering 2004 (IEEE Cat. No.04CH37513), 2004

Publication

&lt;1 %

18	N. P. SINGH, Y. P. SINGH. "Power system excitation and governor control design via time-scale decomposition", International Journal of Systems Science, 1988 Publication	<1 %
19	repository.ubn.ru.nl Internet Source	<1 %
20	Submitted to Liverpool John Moores University Student Paper	<1 %
21	N. C. PAHALAWATHTHA, G. S. HOPE, O. P. MALIK. "MIMO self-tuning power system stabilizer", International Journal of Control, 1991 Publication	<1 %
22	Submitted to Nottingham Trent University Student Paper	<1 %
23	downloads.hindawi.com Internet Source	<1 %
24	people.bath.ac.uk Internet Source	<1 %
25	K. YAMASHITA, K. OKANO, T. TANIGUCHI. "A method of optimization taking into account the non-linearity of the power torque-angle curve for a synchronous machine", International Journal of Control, 2007 Publication	<1 %

---

26

K. Kobravi. "Analysis of Bifurcation and Stability in a Simple Power System Using MATCONT", 2007 Canadian Conference on Electrical and Computer Engineering, 04/2007

Publication

<1 %

---

27

K.T. Vu, Chen-Ching Liu, C.W. Taylor, K.M. Jimma. "Voltage instability: mechanisms and control strategies [power systems]", Proceedings of the IEEE, 1995

Publication

<1 %

---

Exclude quotes      Off

Exclude matches      Off

Exclude bibliography      On



# MODELLING OF CHAOTIC BEHAVIOR IN POWER SYSTEMS USING RECURRENT NEURAL NETWORKS

---

GRADEMARK REPORT

---

FINAL GRADE

**/0**

GENERAL COMMENTS

**Instructor**

---

PAGE 1

---

PAGE 2

---

PAGE 3

---

PAGE 4

---

PAGE 5

---

PAGE 6

---